LA-UR-83-3422

CONF-840653--1

Los Alamos National Laboratory is operated by the University of California for the United States Department of Energy under contract W-7405-ENG-36

LA-UR--83-3422

DE84 003818

TITLE: NEW EXPERIMENTAL TECHNIQUES WITH THE SPLIT HOPKINSON PRESSURE BAR

AUTHOR(S): C. E. Frantz, P. S. Follansbee, and W. J. Wright

SUBMITTED TO: 8th International Conference on High Energy Rate Fabrication
June 17-21, 1984 San Antonio, TX

DISCLAIMER

MASTER

Los Alamos National Laboratory
Los Alamos, New Mexico 87545

New Experimental Techniques with the Split Hopkinson Pressure Bar

C. E. Frantz, P. S. Follansbee, and W. J. Wright

Materials Science and Technology Division
Los Alamos National Laboratory
Los Alamos, New Mexico, 87545

Abstract

The split Hopkinson pressure bar or Kolsky bar has provided for many years a technique for performing compression tests at strain rates approaching 10^4 s^{-1}. At these strain rates, the small dimensions possible in a compression test specimen give an advantage over a dynamic tensile test by allowing the stress within the specimen to equilibrate within the shortest possible time. The maximum strain rates possible with this technique are limited by stress wave propagation in the elastic pressure bars as well as in the deforming specimen. This subject is reviewed in this paper, and it is emphasized that a slowly rising excitation is preferred to one that rises steeply. Experimental techniques for pulse shaping and a numerical procedure for correcting the raw data for wave dispersion in the pressure bars are presented.

For tests at elevated temperature a "bar mover" apparatus has been developed which effectively brings the cold pressure bars into contact with the specimen, which is heated with a specially designed furnace, shortly before the pressure wave arrives. This procedure has been used successfully in tests at temperatures as high as 1000 C.

1 Introduction

The interest in mechanical properties at high rates of strain has over the years led to various experimental techniques for measuring these properties. Methods based on the Hopkinson bar generally have emerged as the most popular of these techniques. In this paper we describe some new experimental techniques that have been developed for experiments with the split Hopkinson pressure bar (SHPB). We first will review the use of the Hopkinson bar, as configured for compression testing, and then describe some of the problems associated with

elastic and plastic wave propagation. We also review the analytical work of a number of previous investigators that defines the optimum conditions for a valid SHPB test. In section 2 we describe experimental techniques for achieving these conditions. A numerical correction for wave dispersion is described and demonstrated in section 3. Finally, a new method for performing elevated temperature compression tests in a SHPB is presented in section 4.

1.1 Historical Perspective. The Hopkinson bar derives its name from its originator who early in this century used a single, long, elastic bar to study pressures produced by the impact of bullets [1]. Many years later Davies [2], then Kolsky [3], followed with significant improvements in the experimental techniques. Davies introduced the use of a condenser to measure displacements in the bars. Kolsky introduced the split Hopkinson pressure bar technique and first described how stress and strain within the deforming specimen are related to displacements in the transmitter and incident pressure bars*. The use of strain gages to measure displacements in the pressure bars was first reported by Hauser, Simmons and Dorn [4]. Lindholm proposed further advances in experimental techniques to load in tension [5] and to perform elevated temperature tests [5] and has provided standardized test techniques that are the basis for Hopkinson bar testing today [6,7].

1.2 Wave Propagation. Along with these developments in the experimental techniques has evolved an increase in the understanding of wave propagation. This has been essential since the test techniques involve the propagation of elastic waves in the pressure bars and of elastic and plastic waves in the specimen. Davies [2] analyzed wave propagation in the elastic pressure bar by applying the mathematical solution, derived by Pochhammer [8] and Chree [9], for the vibrational behavior of a semi-infinite cylinder. Among the contributions of Davies' work were the descriptions of dispersive phenomena and of conditions required for planar wave propagation in the pressure bars.

Dispersion of elastic waves in the pressure bars results from the variation of sound velocity with the wavelength of the excitation; these effects have been

* Because of these major contributions the SHPB is often referred to as the Kolsky bar.

described generally [10,11] as well as for the specific configuration of the SHPB [12]. There are at least two consequences of wave disperison that affect the test results. Wave dispersion leads to the appearance of oscillations in the waves, and, because stress and strain in the specimen are deduced from the strain gage records, these oscillations can mask trends in the stress strain curve. Wave dispersion also will tend to broaden a steeply rising wave which is comprised of many short wavelength fourier components; thus a second effect of wave dispersion on the stress strain curve will be the decreased resolution and accuracy in the yield region. These effects are magnified and do not truly represent material behavior due to the extra dispersion that has occurred as the waves propagate from the specimen to the strain gages. A few investigators have concluded that if the strain gages are placed equidistant from the specimen, then disperison effects will cancel. But this is true only if both the reflected wave and the transmitted wave are identical, which is seldom the case. Because the short wavelength fourier components that comprise the leading edge of the incident wave are particularly dispersive, one technique for minimizing the effects of dispersion is to increase the rise time of this wave. In section 2 we will describe some experimental techniques that have this effect. A numerical procedure to correct for the artifical effects of wave dispersion will be presented in section 3.

Elastic wave propagation is now well understood. However, wave propagation within the deforming specimen is far more complicated. It has been emphasized by many previous investigators a valid SHPB test requires a uniform stress throughout the specimen. When the stress wave first enters the specimen, axial and radial inertia oppose the equilibration of stress. Kolsky [3] minimized effects due to axial inertia by using very thin specimens ($l/d \sim 0.1$). Kolsky also derived an approximate correction for radial inertia in the specimen. However, this correction assumed frictionless contact, and it is now generally acknowledged that this condition is difficult to achieve with such thin specimens. Davies and Hunter [13] considered the conditions required for minimization of friction effects and concluded that the l/d ratio should be closer to unity. These investigators also derived a correction for inertial effects and a condition, based on the sound velocity within the specimen and the rise time T, for a valid test. For a plastically deforming metal this requirement is

$$\frac{d\sigma}{d\varepsilon} > \frac{\pi^2 \rho_s d^2}{T^2} , \qquad (1)$$

where ρ_s is the density of the specimen. Davies and Hunter suggested that the test should be rejected when this equality is violated.

The criterion proposed by Davies and Hunter was an attempt to establish conditions for the equilibration of stress. Due to the importance of the uniform stress assumption, numerous investigators have undertaken more complex analyses of plastic wave propagation. Using a one-dimensional analysis, for instance, Jahsman [14] noted discrepancies between the elastic portion of the "reconstituted" and actual stress strain curves. It was also concluded in this study that a trapezoidal stress pulse was preferred to a square-wave pulse, which is consistent with the criteria of eq. (1).

A full two-dimensional numerical analysis was performed by Bertholf and Karnes [15] for the case of an aluminum specimen; it is this work which most thoroughly defines the conditions required for a valid SHPB experiment. These investigators concluded that the effect of friction could be substantial, but that it was systemic (i.e., strain rate independent). Furthermore they concluded that the corrections for inertial effects proposed by Davies and Hunter [13] were reasonable and this this led to an optimum l/d ratio of ~ 0.5. Finally the numerical results led Bertholf and Karnes to propose that, based on inertia, experimental results are valid provided that

$$d\dot{\varepsilon} \leq 5 \times 10^3 \text{ cm-s}^{-1} \qquad (2)$$

and that the excitation is a ramp wave where

$$\frac{T}{d} \geq 16 \text{ μs-cm}^{-1} . \qquad (3)$$

A comparison of eq. (3) with eq. (1) leads to the conclusion that these two conditions are analagous. That is, if eq. (3) is substituted into eq. (1), the minimum value of $d\sigma/d\varepsilon$ is computed to equal 1100 MPa (for aluminum) which is E/65, where E is the elastic modulus, and is a typical value for the initial slope of the stress-plastic strain curve in pure and solution strengthened metals [16]. Thus, it is concluded that account can be made of inertial effects in the

SHPB experiment and that the approximate expressions proposed by Davies and Hunter are remarkably useful.

In this section some complexities associated with wave propagation have been reviewed. In particular, a slow rise time pulse has been shown to be preferable to a steeply rising pulse in order to allow for inertial effects as well as to minimize some of the effects of wave dispersion. With this background, we will turn to a description of some new experimental techniques for the SHPB test. These procedures have been developed to counter the effects of wave propagation and to yield reliable test results, particularly at higher strain rates. We begin with a general description of the test facility in the Materials Science and Technology Division at Los Alamos National Laboratory.

2 Experimental Techniques

The test facility and its operation, including associated hardware and instrumentation, is described in this section. Also discussed are unique procedures such as techniques for wave shaping.

2.1 The Test Apparatus. The test apparatus, illustrated in Fig. 1, consists of a gas gun for propelling the striker bar toward the incident bar, the two pressure bars, and the associated mounting and alignment hardware. This specific apparatus was originally constructed by General Motors Defense Research Laboratories and has been described by Malden and Green [17]. However it has undergone substantial modification since being delivered to Los Alamos National Laboratory. The entire device is mounted on a 8 m long I-beam for stability. The gas gun is 2.6 m long, has a 2.54 cm diameter bore, is equipped with a massive breech, and is supported at four points with adjustable brackets for alignment.

Pressure bars are constructed from maraging steel, heat treated to a yield stress of 2500 MPa and centerless ground. Nominal 4.7 mm, 6.3 mm and 9.2 mm diameter bars have been used and a length to diameter ratio of 125 is typically maintained. Striker bars are cut from identical material to lengths varying from 2.5 cm to 40 cm. For tests with the 9.2 mm diameter bars, two polycarbonate

cylinders with a length and diameter of 2.54 cm are drilled slightly subsized and press fit onto the ends of the striker bars. These shoes guide the striker down the axis of the gun and provide a seal between the high pressure and atmospheric gases. For tests with the smaller diameter pressure bars, a single plastic shoe of the same diameter but up to 10 cm long is used with a single 10 mm diameter hole drilled along the axis but not the full length of the shoe. Small rings of 10 mm outer diameter and the inner diameter determined by the bar size are press fit onto the striker bar. Upon firing the entire assembly is propelled down the gun but before impact with the incident bar the shoe is stopped while the striker bar continues along the axis and alone strikes the incident bar.

2.1.1 Alignment. Precise alignment is critical for a valid test, yet the entire support system must facilitate the removal and replacement of the pressure bars and must not over constrain radial or longitudinal displacements in the pressure bars. The bar mounting system employed is shown in Fig. 2. Each pressure bar is mounted in 7.6 cm x 7.6 cm x 5.1 cm aluminum blocks spaced 20 cm to 30 cm apart and in turn mounted on a 7.6 cm x 7.6 cm by 1.22 m long aluminum bed which is clamped to the I-beam. When the smaller diameter pressure bars are used only one large aluminum bed is required. The smaller mounts are aligned to the bed through a series of precision machined 1.27 cm wide grooves in the bed and blocks and a square peg as illustrated in Fig. 2. The pressure bars slide through oilite bushings precisely mounted in the aluminum mounts. The diameter of the hole through the bushing is machined to within .025 mm over the final bar diameter.

Final alignment of the gas gun and of the long aluminum beds is performed with a bore scope mounted on the free end of the I-beam. A target upon which to focus is first placed at various positions along the gun bore and then within one of the small mounting brackets at various positions along the aluminum bed. Adjustment of the clamps and the use of shims leads eventually to optimum alignment. Once this procedure is complete, the bars can be removed and replaced without disrupting the alignment.

2.1.2 Bar Dimensions and Lubrication. As described by a number of previous investigators, errors due to both radial and longitudinal inertia and to friction are reduced by minimizing the area mismatch at the sample-pressure bar

interface and by maintaining a sample length to diameter ratio of 0.5 to 1. Typically the sample diameter is machined to 80% of the bar diameter, which allows around 30% true strain before the bar diameter is exceeded. A length to diameter ratio of 0.6 is specified for most experiments.

For the room temperature experiments a molybdenum disulfide lubricant is typically used at the sample-bar interface. The thickness of the grease film must be minimized; failure to do this can lead to errors in the strain measurement as well as to uncertain timing between the various waves due to the extrusion of lubricant during the test.

2.1.3 Instrumentation and Data Acquisition. Strain gages are used as sensors for the Hopkinson bar tests. They are mounted in pairs, at diametrically opposite positions, at the midlength of the incident and transmitter bars. Paper back gages available from BLH have been used successfully. These gages are pliable, conform readily to the bar curvature, and can be attached with Duco cement. The most difficult part of the procedure is the installation and attaching of the lead wires, and failure of the gages most often occurs in this region. Figure 3 is a photograph of a strain gaged bar assembly. Leads are 28 gauge insulated copper wire and are lashed to the bar with monofilament nylon line. A short exposed piece of the lead wire is soldered to the internal gage lead wire. Arching of the lead wire (see Fig. 3) seems to add tolerance to the strong stress waves in the bars.

Standard Wheatstone bridge circuitry is used with the gages. The output of the bridge is fed through a low noise differential amplifier with a bandwidth greater than 1 MHz. The amplifier outputs are recorded by Biomation 1010 digital transient recorders (10 MHz sampling rate, 10 bit resolution). The use of digital recorders simplifies the significant problem of establishing timing relationships between the waves since the time bases of the two recorders can be precisely correlated through digital triggering and delay.

Once the strain gage traces are captured with the transient recorders, the data can be transferred to and processed by a desk top computer and stored on magnetic media. The calculation of stress and strain from the strain gage signals requires knowledge of the longitudinal sound velocity and elastic modulus

in the pressure bars; these are obtained from independent ultrasonic measurements. Wave propagation times for large amplitude excitations also have been measured in the bars and generally lead to estimates of the sound velocity which exceed those from the ultrasonic measurements by 1/2 % to 1%.

2.2 Wave Shaping. In section 1 some of the errors arising from wave propagation in the pressure bars and the specimen were described, and it was pointed out that a slowly rising incident wave is preferred to a sharply rising wave. The rise time increases naturally during propagation due to wave dispersion. However, there are far more effective ways to increase the rise time of the leading edge of the incident wave. A standard technique is to machine a large radius on the input face of the striker bar; we typically specify a radius of 8.9 cm. This produces a slightly non-planar inpact condition at the striker bar-incident bar interface, but these effects become insignificant a short distance from this interface.

Another effective technique for increasing the rise time of the incident wave is to place a "tip material" between the striker bar and incident bar. The tip material is a disc slightly larger in diameter than the bar and 0.1 mm to 2 mm in thickness. It can be made from paper, aluminum, copper, brass, stainless steel, etc. and is often the same material as the sample. The disc is attached to the impact face of the incident bar. Upon impact it yields and softens the initial impact, leading to an increase in the rise time. Unfortunately the choice of tip material and its thickness is often a trial and error process.

A properly chosen tip material can also be used to generate a constant strain rate experiment. A simple impact between a striker bar and the incident bar produces a square wave of approximately constant stress. However as the sample work hardens and as it increases in diameter the strain rate typically decreases rapidly which is undesireable when fundamental material properties or constitutive relations are being investigated. Shaping the incident wave to yield an increasing stress can be used to produce a more uniform strain rate. In fact, Ellwood et al [18] have demonstrated that a three bar system with identical samples sandwitched between the bars will yield such a result. We have not found it necessary to add a third pressure bar, although this method might remove the guesswork from the choice of a tip material and likely would be more effective at

low strain rates and large strains where the use of a tip material has been found to be insufficient to produce a constant strain rate during the entire test. An example of the effect of a tip material on the shape of the incident wave and of the resulting strain rate is shown in Fig. 4. A 0.7 mm thick brass disc was used in this experiment on annealed 3041 stainless steel at a strain rate of 4500 s^{-1}.

At very high strain rates the stress levels in the incident wave far exceed those in the sample and thus relatively small changes in the strength of the sample have little influence on the strain rate. The true strain rate is often quite uniform in these experiments. However at these strain rates the use of a tip material to increase the rise time of the incident wave is essential.

3 Dispersion Correction

In the previous section techniques for pulse shaping were described. An additional benefit of pulse shaping is that increasing the rise time of the leading (and trailing) edge of the wave reduces the amplitude of the high frequency components within the wave which disperse readily. This is evident is Fig. 4; the strain rate curve for the case of a tip material contains lower amplitude oscillations than when no tip material was used.

As described in section 1 wave dispersion can mask trends in the stress strain curve, particularly at high strain rates where the period of the oscillations can be a large fraction of the duration of the test. Wave dispersion can not be eliminated, but techniques have been developed to correct for any additional disperion that occurs during travel from the specimen-pressure bar interfaces to the strain gages. The technique, which has been described in detail by Follansbee and Frantz [19] and used earlier by Gorham [20], will be briefly reviewed below.

At any position z along the bar the wave f(t) can be represented by the infinite cosine series

$$f(t) = \frac{A_o}{2} + \sum D_n \cos (n\omega_o t - \delta_n) \qquad (4)$$

where ω_o is the frequency of the longest wavelength component (n = 1) and δ_n is the phase angle of component $n\omega_o$. Wave dispersion occurs in long cylindrical

bars because the higher frequency components travel more slowly than lower frequency components and thus lag behind the leading edge of the wave. Dispersion affects the value of the phase angle δ; at a position $z + \Delta z$, the new phase angle is

$$\delta(z + \Delta z) = \delta(z) + \frac{n\omega_o \Delta z}{C_o}\left(\frac{C_o}{C_n} - 1\right) \qquad (5)$$

where C_o is the velocity of an infinitely long component (the longitudinal sound speed) and C_n is the velocity of component $n\omega_o$. The value of C_n depends on the wavelength and on the mode of vibration and can be determined analytically. For conditions of Hopkinson bar experiments, Davies [2] concluded that the fundamental mode dominated vibration; this was verified in [19]. Thus the phase angle at any new position can be computed from equation (5) and the wave reconstructed at that new position according to equation (4).

Actually the Pochhammer-Chree solution of the equation of motion for an infinitely long cylinder leads to a correspondence between C_n/C_o and R/λ_n where R is the bar radius and λ_n is the wavelength of component $n\omega_o$. For the fundamental mode of vibration C_n/C_o decreases from 1 at $r/\lambda = 0$ to 0.57 at $R/\lambda > 1$. Thus for a given wavelength, R/λ decreases with decreasing bar diameter. This implies that the velocity of that component will increase with decreasing bar diameter which will decrease the effects of dispersion and is one reason why smaller pressure bars are desireable for the higher strain rate tests.

To demonstrate the effectiveness of the dispersion correction procedure described above the following experiment was performed. A single 2 m long pressure bar was instrumented with two sets of strain gages at points 0.5 m from the impact end (position 1) and 1.0 m from the impact end (position 2), which are the typical locations of the incident bar strain gage and sample respectively. A striker bar was impacted with the pressure bar and the strain gage signals recorded as described previously. Figure 5a shows a comparison of the measured wave at position 1 with the wave measured at position 2 and moved (corrected) back to position 1. Likewise, Fig. 5b compares the wave measured at position 2 with that measured at position 1 and moved up to position 2. It is evident in these figures that the correction forward (Fig. 5b) is slightly better than the correction backward (Fig. 5a). However in both cases the correction describes

the major features of wave dispersion and deviations between the correction and actual dispersion is in the finer details.

The effect of the dispersion correction on the appearance of a stress strain curve is shown in Fig. 6 for a stainless steel sample (annealed Nitronic 40) tested at a strain rate of $5x10^3$ s^{-1}. In this case the correction has yielded a much smoother stress strain curve that is easier to interpret than the uncorrected curve.

4 High Temperature Testing

The extension of Hopkinson bar techniques to elevated temperature poses several problem. Because the stress and strain within the deforming specimen are determined from strain gage measurements on the elastic pressure bars, which depend on the elastic modulus and sound velocity of the bar material, the temperature of the pressure bars is important. One technique for elevated temperature testing might be to uniformly heat the pressure bar and specimen assembly. However, this would necessitate refractory metal pressure bars for temperatures greater than about 600 C and would require new strain gage technology.

A number of investigators have placed a furnace around the specimen and a portion of the pressure bars and have allowed heat conduction through the bars. This leads to a temperature gradient along the pressure bars and thus to a sound velocity and an elastic modulus gradient that will distort the elastic wave. If the temperature gradient is known, the strain gage records can be corrected for these effects. Such corrections have been described by Lindholm and Yeakley [5], Chiddister and Malvern [21], and Sierakowski, Malvern, and Ross [22].

We have developed a new technique for performing high temperature compression tests with the split Hopkinson pressure bar. In this procedure, only the sample is heated within a specially designed furnace assembly; the pressure bars initially are separated from the specimen and kept cool. When the test is initiated, the pressure bars are brought into contact with the specimen an instant before the wave passes through. The intent is to limit contact such that

there is insufficient time for heat flow from the specimen to significantly reduce the specimen temperature.

A schematic of the furnace and furnace housing is shown in Fig. 7. The furnace housing is a small vacuum chamber with double O-ring seals through which the pressure bars pass. A film of molybdenum disulfide grease on the bars lubricates the seals. Pressures of 10^{-6} torr are typically obtained with the diffusion pumping system.

The furnace is constructed from a 1.91 cm diameter by 3.18 cm long piece of boron nitride with a 1.11 cm diameter hole drilled through its center. Molybdenum heating wire is threaded through twenty-three 0.76 mm diameter holes that are drilled along hole circles of 17 mm and 21 mm.

The sample, which for these tests is typically 7.62 mm in diameter by 7.62 mm long, is supported by two "L" shaped rings extruded from 51 μm thick sheets of tantalum or copper. These supports are strong enough to support the specimen yet weak enough to not interfere with the diametrial expansion of the specimen during compression. Between the sample and the pressure bars are mounted several layers (4 to 6 depending on the test temperature) of 2.5 μm thick nickel radiation shields. The three outermost shields, located near the end of the furnace, are slit radially such that the pressure bars can pass through unimpeded. The remaining layers, located directly adjacent to the specimen, are sandwiched at the pressure bar-specimen interface. Room temperature tests in the furnace configuration with and without these radiation shields have indicated that the presence of these shields has no effect on the resulting measurements. A thin layer of fine boron nitride powder is used as a lubricant at the specimen interface.

At the beginning of a test the ends of the pressure bars are precisely located just inside the furnace housing but outside the actual furnace. The desired temperature is set and measured with a thermocouple in the hot section of the furnace. When ready, the bar mover rapidly slides the bars through the first radiation shields and into the furnace. The bar mover is a screw drive with opposing threads on each end. An electric motor drives the screw with a chain linkage. Two arms connect the screw drive to the pressure bars. When the arm

connected to the transmitter bar passes a carefully positioned switch consisting of a light and photodiode the gas gun is triggered. The switch is set such that the bars are in contact with the specimen for 50 ms to 150 ms before the compression wave enters the specimen. Separate tests with an instrumented specimen have indicated less than 5 C decrease in sample temperature for contact times up to 400 ms. In these experiments the contact time is the difference between the time of zero bar velocity and the arrival of the incident wave; the former is measured with a velocity transducer on the arm driving the transmitter bar.

An example of a 1000 C test of iridium at a strain rate of 4500 s^{-1} is shown in Fig. 8. The data in Fig. 8 indicate that an advantage of the procedure described in this section over other elevated temperature test configurations is the temperature capability. Although 1000 C is the highest temperature tested to date in this facility, still higher temperatures are possible.

5. Summary

Several new experimental techniques for testing with the split Hopkinson pressure bar have been described in this paper. With the exception of the elevated temperature testing technique described in the previous section, these procedures have been designed to counter effects of wave propagation. It has been emphasized that the rise time of the incident wave can critically affect the test results. Although the benefits of a slowly rising wave over a steeply rising wave in promoting the equilibration of stress within the deforming specimen have been described previously [13,15], a contribution of this work has been to show how this rise time can be adjusted experimentally.

An increased rise time in the incident wave also will reduce the magnitude of the short wavelength fourier components in the wave which disperse more readily and thus will lead to a more reliable measurement. However, wave dispersion can still become a problem at the highest strain rates. When this is the case, a numerical procedure, described in section 3, can be applied to correct for any "extra" dispersion due to wave propagation from the specimen to the strain gages.

One question that is of continued interest involves the limits, particularly in regard to the strain rate, of the SHPB test technique. A criterion proposed by Bertholf and Karnes [15] was given in eqs. (2) and (3). However, this criterion was based on a specific set of calculations for an aluminum specimen. It is likely that for a lower work hardening material (which implies a lower sound velocity) eq. (2) would be too optimistic. On the other hand, inspection of the actual comparisons in [15] might lead one to conclude that eq. (2) is too restrictive. Clearly, additional calculations that specifically investigate the effects of strain rate and the shape of the stress strain curve would help answer this question.

Inspection of eqs. (2) and (3) suggests that the maximum strain rate in a SHPB test is limited only by the ability to construct smaller diameter pressure bars and specimens. In practice this is not the case due to uncertainty in the timing between the incident and reflected waves. Even when the strain gages on the pressure bars are equidistant from the specimen-pressure bar interface, the reflected and transmitted waves do not arrive at the records at the same instant. The transmitted wave typically lags behind the incident wave due to i) transit time through the specimen and ii) transit time at the imperfect interfaces. The former effect does scale with the specimen dimensions, but the latter does not; it is rather a function of the specimen preparation and lubrication techniques. The uncertainty in the time relationships of the waves can be on the order of 2 μs, which becomes significant as the strain rate increases. To see this, note that for a test at an average strain rate of 10^4 s^{-1} to a strain of 0.2, the duration of the entire test is only 20 μs. Thus, although inertia effects can be minimized through adherence to eq. (1) and through appropriate choice of bar size and the use of wave shaping, the uncertainties in the timing of the waves used to construct a stress strain curve can in practice limit the maximum strain rate in a SHPB test.

The SHPB test has gained popularity because mechanical properties at high strain rates can be investigated without incorporating into the data reduction procedure details of wave propagation. That is, the stress within the specimen is assumed to be uniform at any instant. When higher strain rates are desired, the experimental techniques must involve non-uniform deformation that significantly complicates the analysis. The Taylor test [23] and the flyer plate

impact test (see, for example [24]) are examples of experiments involving higher rates of deformation than possible in the SHPB but which involve complicated stress wave phenomena. It has been emphasized in this paper, however, that wave propagation does influence the SHPB test and that a proper understanding of these effects is required in order to establish conditions for test validity and strain rate limitations.

Acknowledgement

This work has been performed under the auspices of the U. S. Department of Energy. The authors also wish to extend their gratitude to Phil Armstrong who provided helpful suggestions throughout this work.

References

1 Hopkinson, B., "A Method of Measuring the Pressure Produced in the Detonation of High Explosives or by the Impact of Bullets," Philosophical Transactions A, Vol. 213, 1914, pp. 437-456.

2 Davies, R. M., "A Critical Study of the Hopkinson Pressure Bar," Philosophical Transactions A, Vol. 240, 1948, pp. 375-457.

3 Kolsky, H., "An Investigation of the Mechanical Properties of Materials at Very High Rates of Loading," Proceedings of the Physical Society B, Vol. 62, 1949, pp. 676-700.

4 Hauser, F. E., Simmons, J. A. and Dorn, J. E., "Strain Rate Effects in Wave Propagation," in Response of Metals to High Velocity Deformation, Metallurgical Society Conferences, Vol. 9, P. G. Shewmon and V. F. Zackay, Ed., Interscience, New York, 1961, pp. 93-110.

5 Lindholm, U. S. and Yeakley, L. M., "High Strain-Rate Testing: Tension and Compression," Experimental Mechanics, Vol. 8, 1968, pp. 1-9.

6 Lindholm, U. S., "Some Experiments with the Split Hopkinson Pressure Bar," Journal of the Mechanics and Physics of Solids, Vol. 12, 1964, pp. 317-335.

7 Lindholm, U. S., "High Strain Rate Tests," in Measurement of Mechanical Properties, Vol. V, Part 1, R. F. Bunshah, Ed., Interscience, New York, 1971, Chap. 4, pp. 199-271.

8 Pochhammer, L., "On the Propagation Velocities of Small Oscillations in an

Unlimited Isotropic Circular Cylinder," Journal fur die Reine und Angewandte Mathematik, Vol. 81, 1876, pp. 324-326.

9 Chree, C., "The Equations of an Isotropic Elastic Solid in Polar and Cylindrical Coordinates, Their Solutions and Applications," Cambridge Philosophical Society, Transactions, Vol. 14, 1889, pp. 250-369.

10 Kolsky, H., Stress Waves in Solids, Dover Publications, New York, 1963.

11 Curtis, C. W., "Propagation of an Elastic Pulse in a Semi-Infinite Bar," in International Symposium on Stress Wave Propagation in Materials, N. Davids, Ed., Interscience, New York, 1960, pp. 15-43.

12 Yeung Wye Kong, Y. C. T., Parsons, B. and Cole, B. N., "The Dispersive Behavior of a Hopkinson Pressure Bar in Material Property Tests," in Mechanical Properties at High Rates of Strain, Institute of Physics Conference Series No. 21, 1974, pp. 33-47.

13 Davies, E. D. H. and Hunter, S. C., "The Dynamic Compression Testing of Solids by the Method of the Split Hopkinson Pressure Bar," Journal of the Mechanics and Physics of Solids, Vol. 11, 1963, pp. 155-178.

14 Jahsman, W. E., "Reexamination of the Kolsky Technique for Measuring Dynamic Material Behavior," ASME Journal of Applied Mechanics, Vol. 38, 1971, pp. 75-82.

15 Bertholf, L. D. and Karnes, C. H., "Two-Dimensional Analysis of the Split Hopkinson Pressure Bar System," Journal of the Mechanics and Physics of Solids, Vol. 23, 1975, pp. 1-19.

16 Kocks, U. F., "Strain Hardening and 'Strain-Rate Hardening'," in Mechanical Testing for Deformation Model Development, ASTM STP 765, R. W. Rohde and J. C. Swearengen, Eds., American Society for Testing and Materials, 1982, pp. 121-138.

17 Malden, C. J. and Green, S. J., "Compressive Strain-Rate Tests on Six Selected Materials at Strain Rates from 10^{-3} to 10^{4} in./in./sec," ASME Journal of Applied Mechanics, Vol. 33, 1966, pp. 496-504.

18 Ellwood, S., Griffiths, L. J. and Parry, D. J., "Materials Testing at High Constant Strain Rates," Journal of Physics E: Scientific Instrumentation, Vol. 15, 1982, pp. 280-282.

19 Follansbee, P. S. and Frantz, C. E., "Wave Propagation in the Split Hopkinson Pressure Bar," ASME Journal of Engineering Materials and Technology, Vol. 105, 1983, pp. 61-66.

20 Gorham, D. A., "Measurement of Stress-Strain Properties of Strong Metals at

Very High Rates of Strain," in Mechanical Properties at High Rates of Strain, J. Harding, Ed., Institute of Physics Conference Series No. 47, 1979, pp. 16-24.

21 Chiddister, J. L. and Malvern, L. E., "Compression-Impact Testing of Aluminum at Elevated Temperatures," Experimental Mechanics, Vol. 3, 1963, pp. 81-90.

22 Sierakowski, R. L., Malvern, L. E. and Ross, C. A., "Compression Testing of Metals at Elevated Temperatures," AFATL-TR-80-76, United States Air Force Armament Laboratory, 1980.

23 Taylor, G. I., "The Use of Flat-Ended Projectiles for Determining Dynamic Yield Stress. I Theoretical Considerations," Proceedings of the Royal Society A, Vol. 194, 1948, pp. 289-299.

24 Davison, L. and Graham, R. A., "Shock Compression of Solids," Physics Reports, Vol. 55, No. 4, 1979, pp. 255-379.

Figure Captions

Fig. 1. Overall view of the Hopkinson bar with the gas gun at the far end and the bore scope and bar stopper at the rear end.

Fig. 2. Bar mount showing a bearing recessed in a mounting block, the tie-down clamp, mounting bed, and the alignment slots with a square peg.

Fig. 3. A strain gage and lead wire assembly installed on a bar. Underneath the black tape is additional lashing with monofilament nylon.

Fig. 4. Comparison of tests on 3041 stainless steel using no tip material (dashed line) and using 0.7 mm brass tip material (solid line): (a) shows the incident waves while (b) shows the resulting strain rate curves. In (a) one time index point equals 0.1 μs and channel number is proportional to strain.

Fig. 5. Demonstration of the dispersion correction. Upper curves: waves at 0.5 m (solid line) versus wave measured at 1.0 m and corrected to 0.5 m. Lower curves: wave at 1.0 m (dashed line) versus wave measured at 0.5 m and corrected to 1.0 m. One time index point equals 0.1 μs.

Fig. 6. Comparison of the stress-strain curve in Nitronic 40 with (solid curve) and without (dashed curve) the dispersion correction.

Fig. 7. Schematic drawing of the furnace configuration showing the bars, furnace housing, heating element, shields, sample support, and sample.

Fig. 8. Stress-strain curve (solid line) and strain rate versus strain curve for iridium at 1000 C.

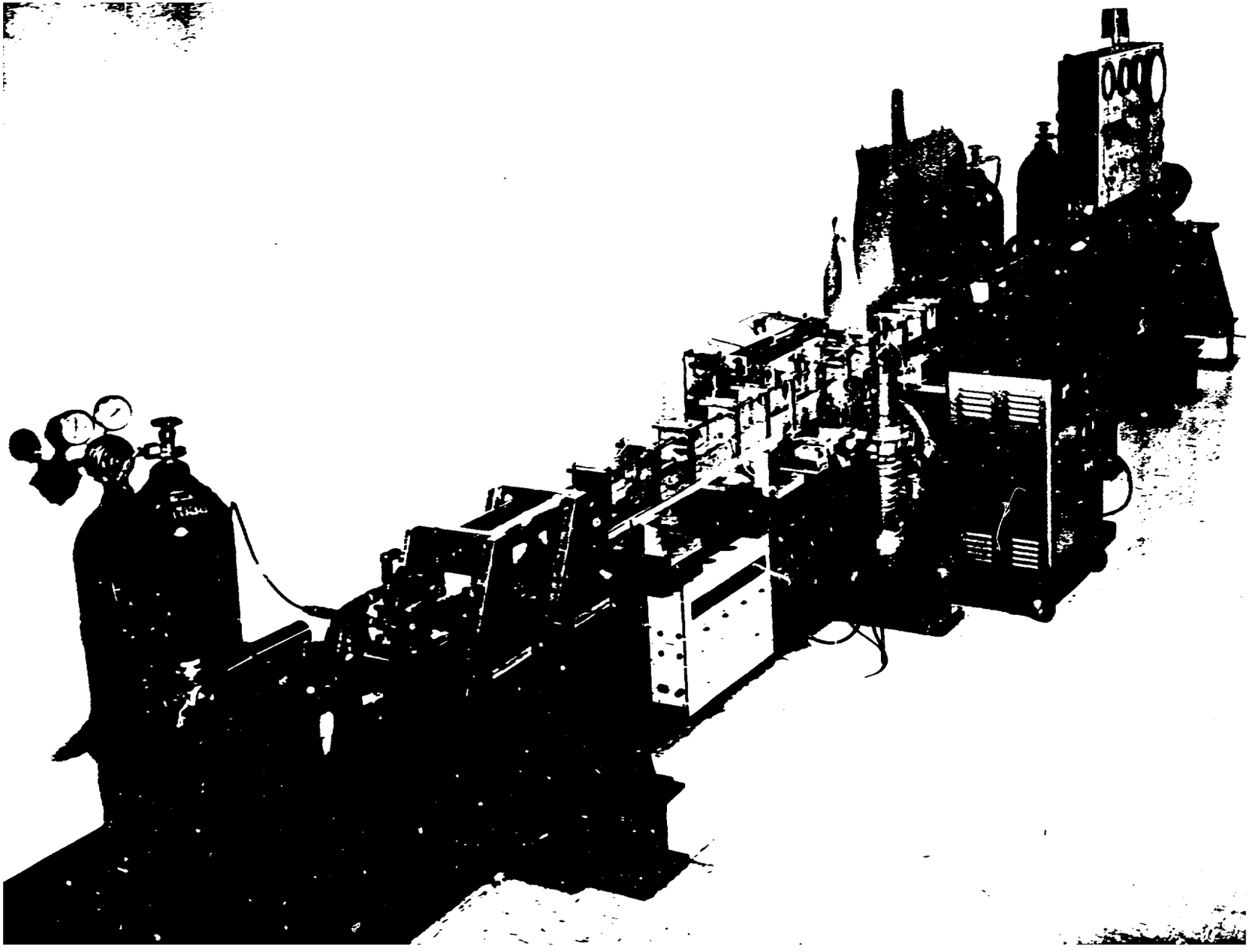

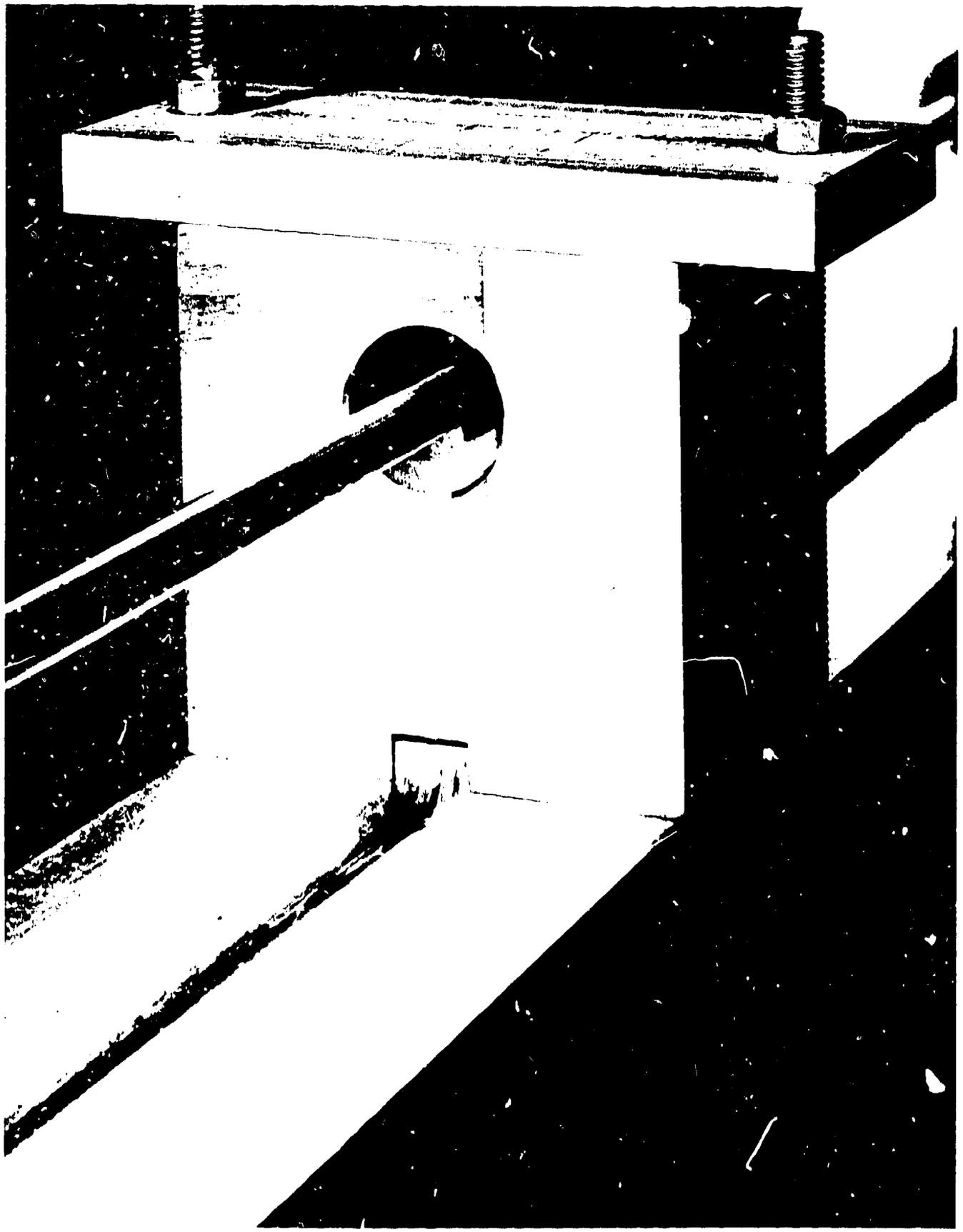

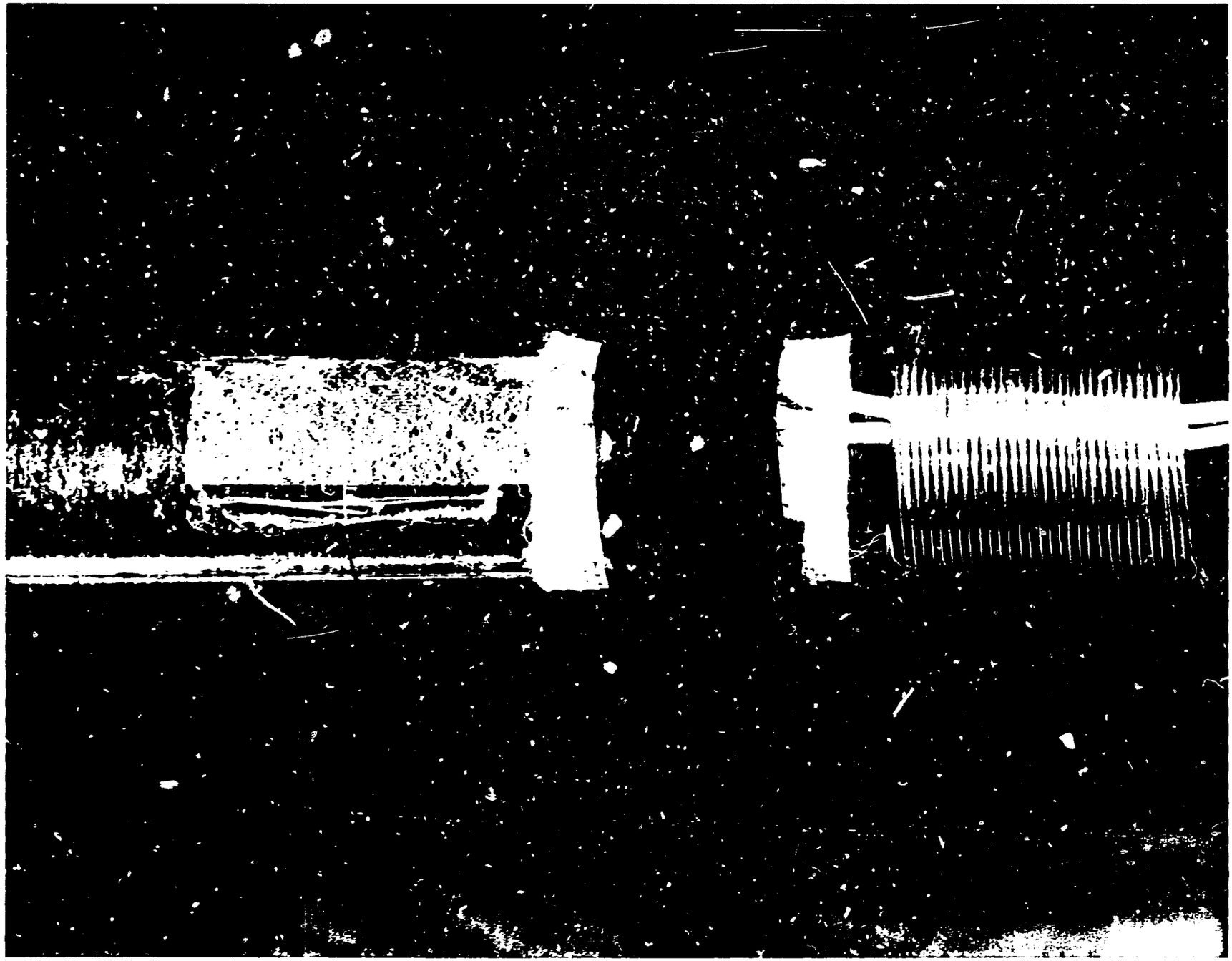

Fig. 4a

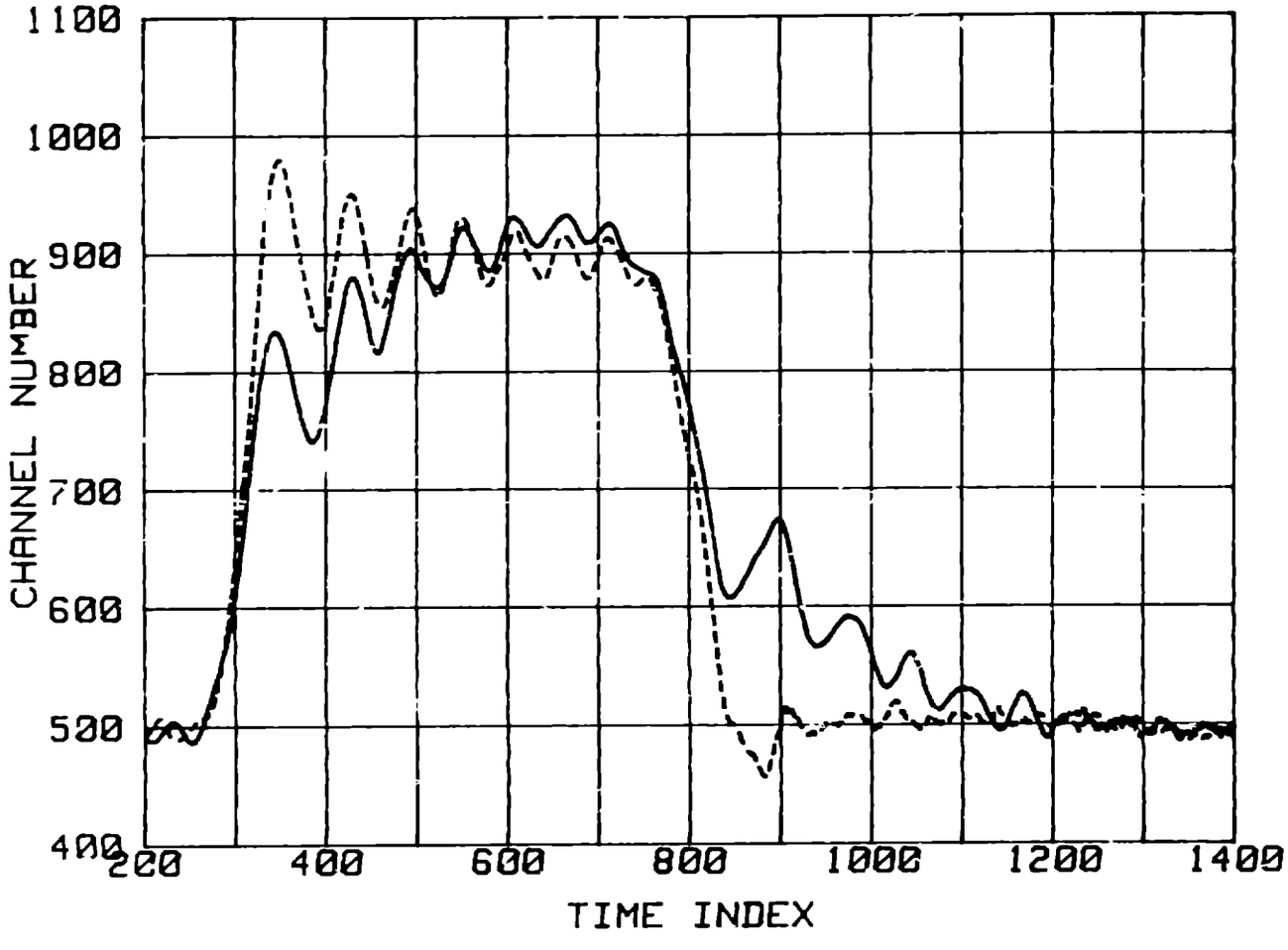
1100
1000
900
800
700
600
500
400
CHANNEL NUMBER
200
400
600
800
1000
1200
1400
TIME INDEX

Fig. 46

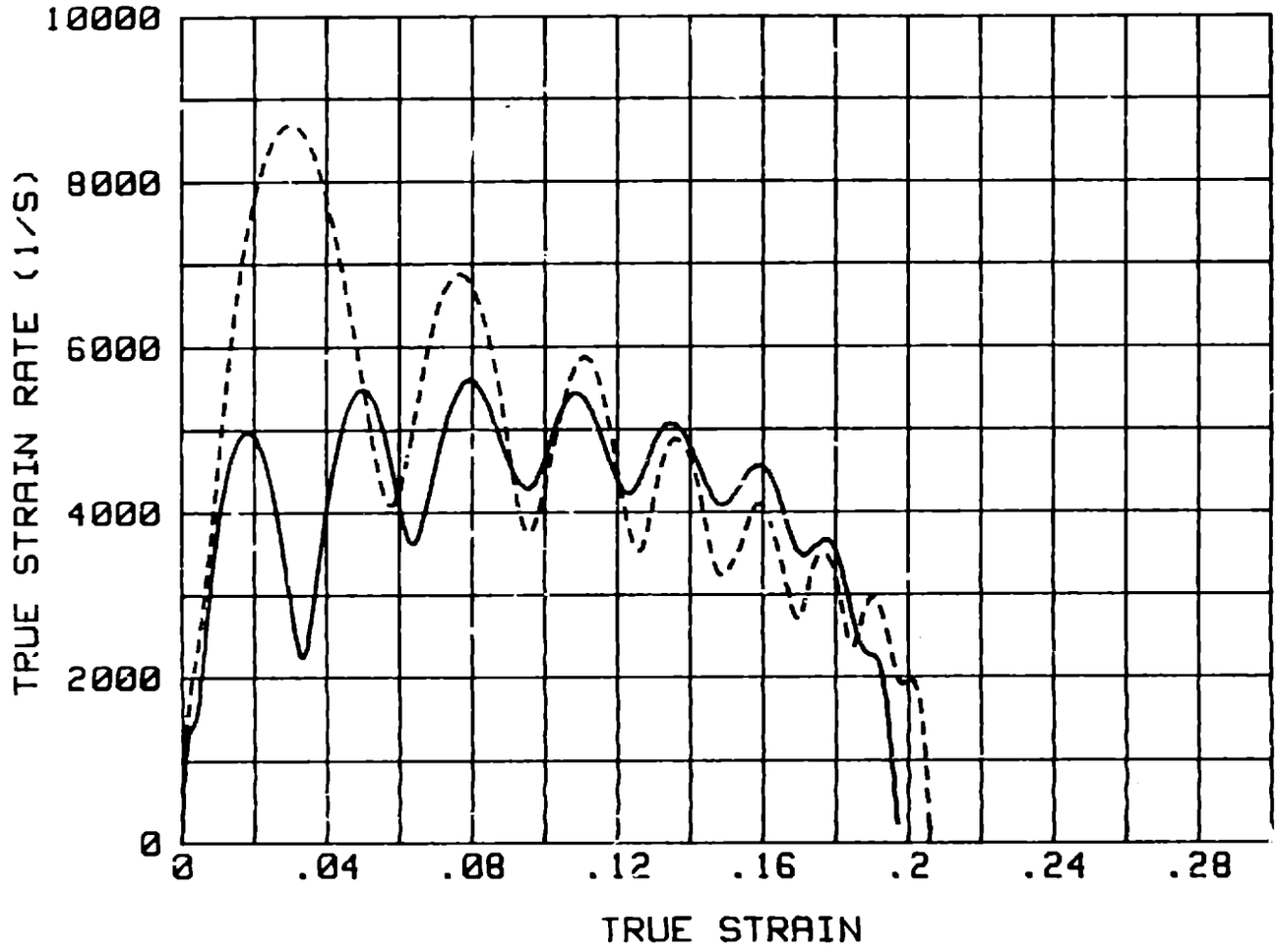
10000
8000
6000
4000
2000
0
TRUE STRAIN RATE (1/S)
0
.04
.08
.12
.16
.2
.24
.28
TRUE STRAIN

Fig. 5

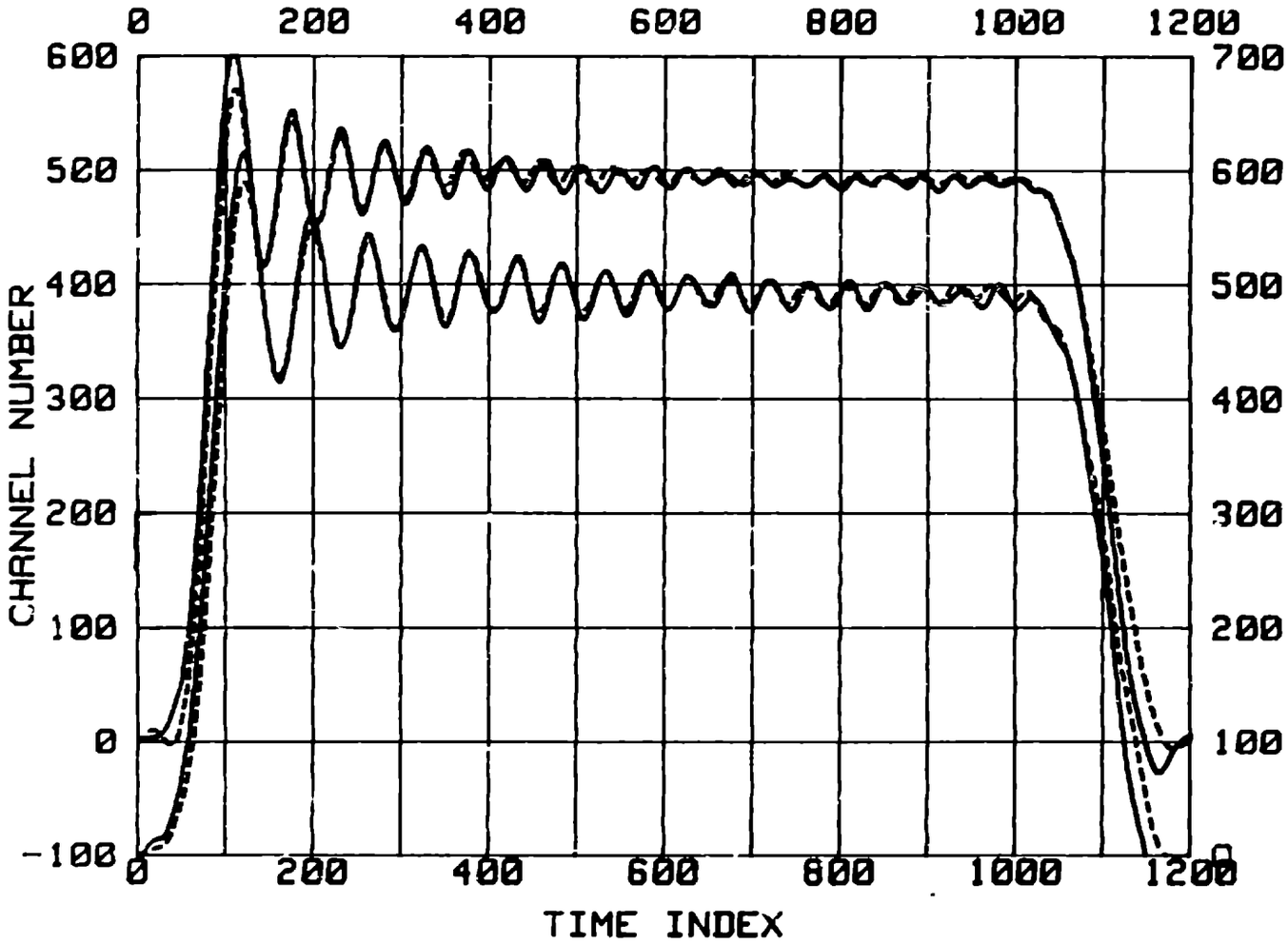
0
200
400
600
800
1000
1200
600
500
400
300
200
100
0
-100
700
600
500
400
300
200
100
0
CHANNEL NUMBER
TIME INDEX

Fig. 6

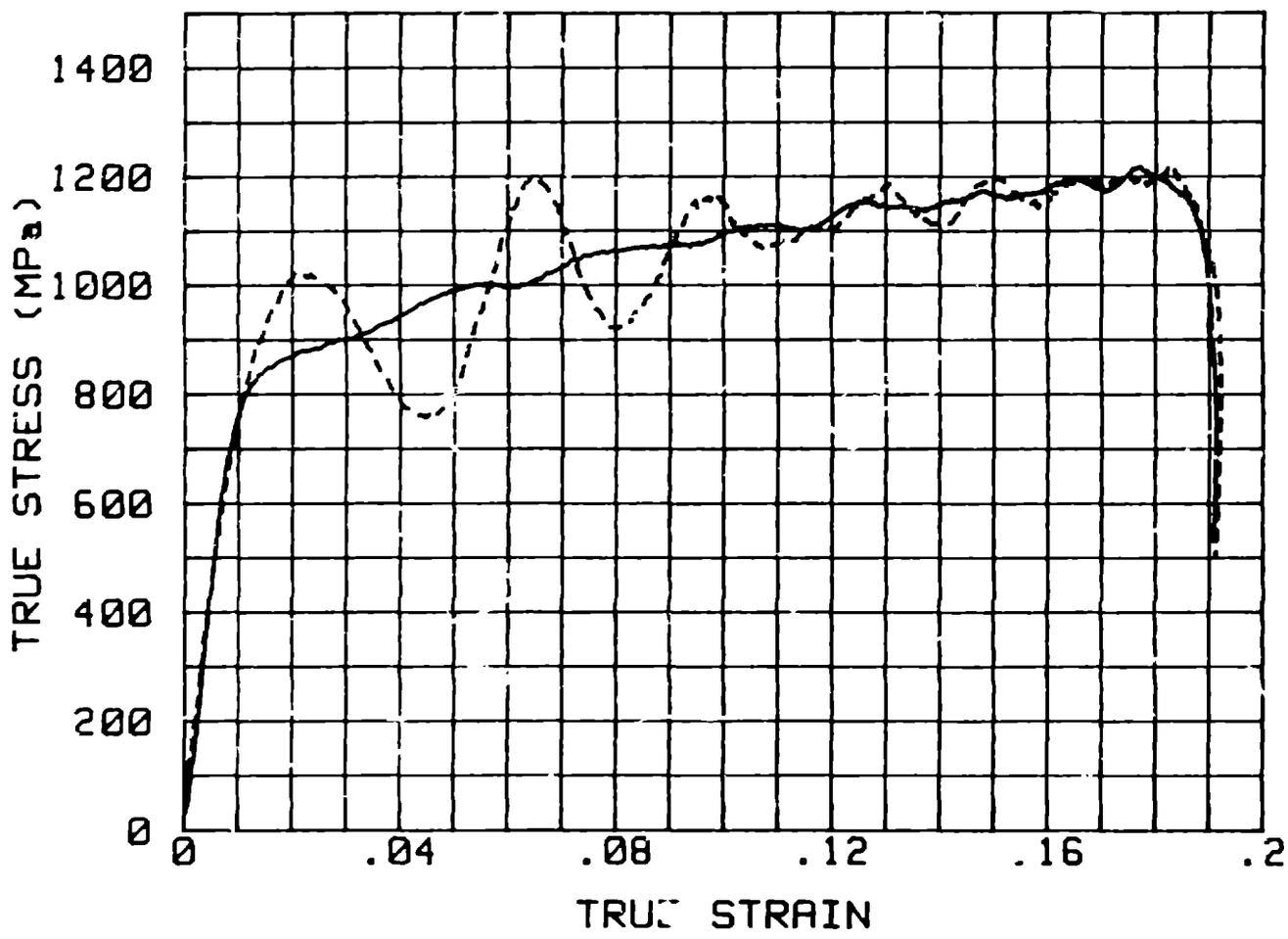
1400
1200
1000
800
600
400
200
0
TRUE STRESS (MPa)
0
.04
.08
.12
.16
.2
TRUE STRAIN

Fig. 7

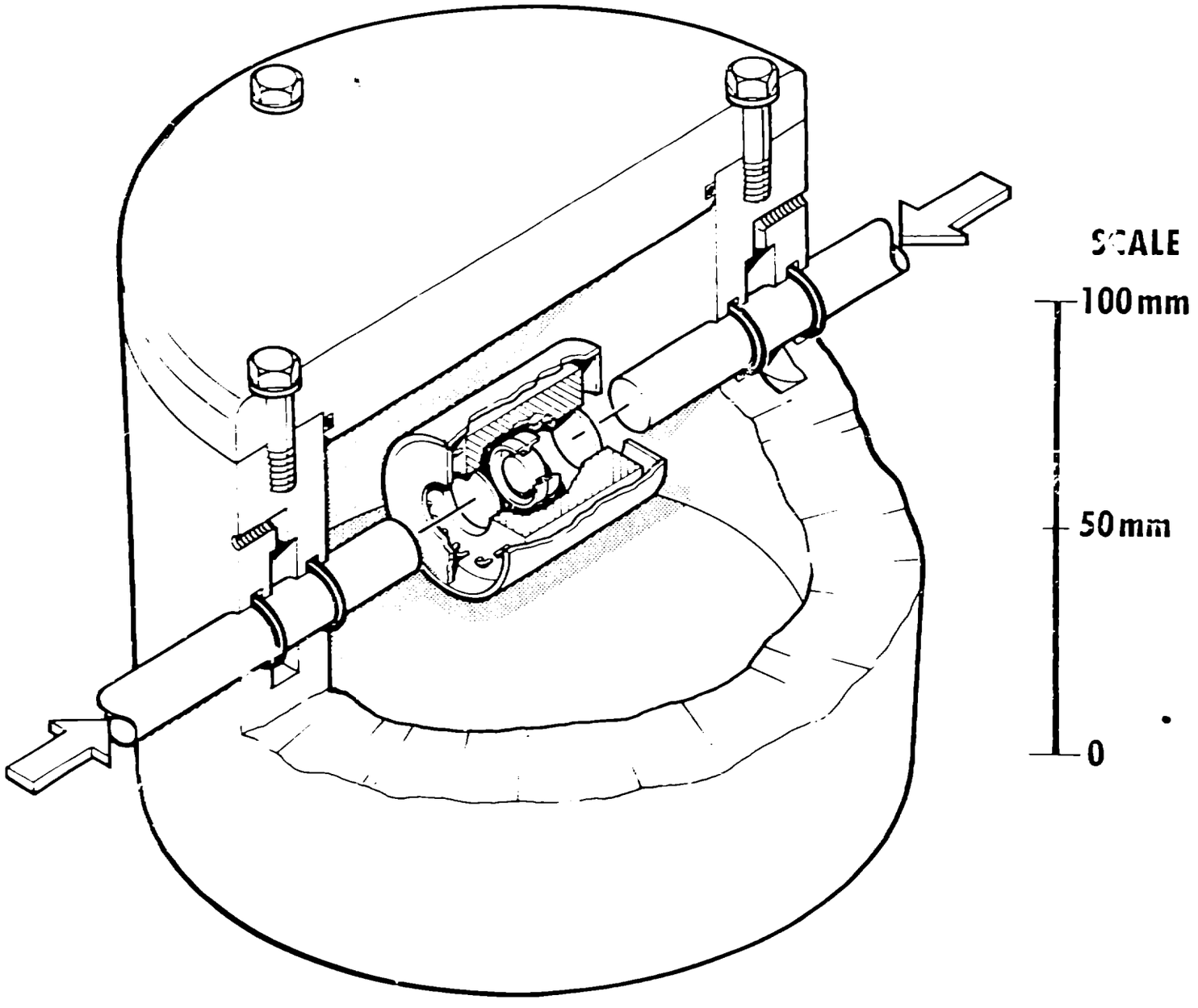

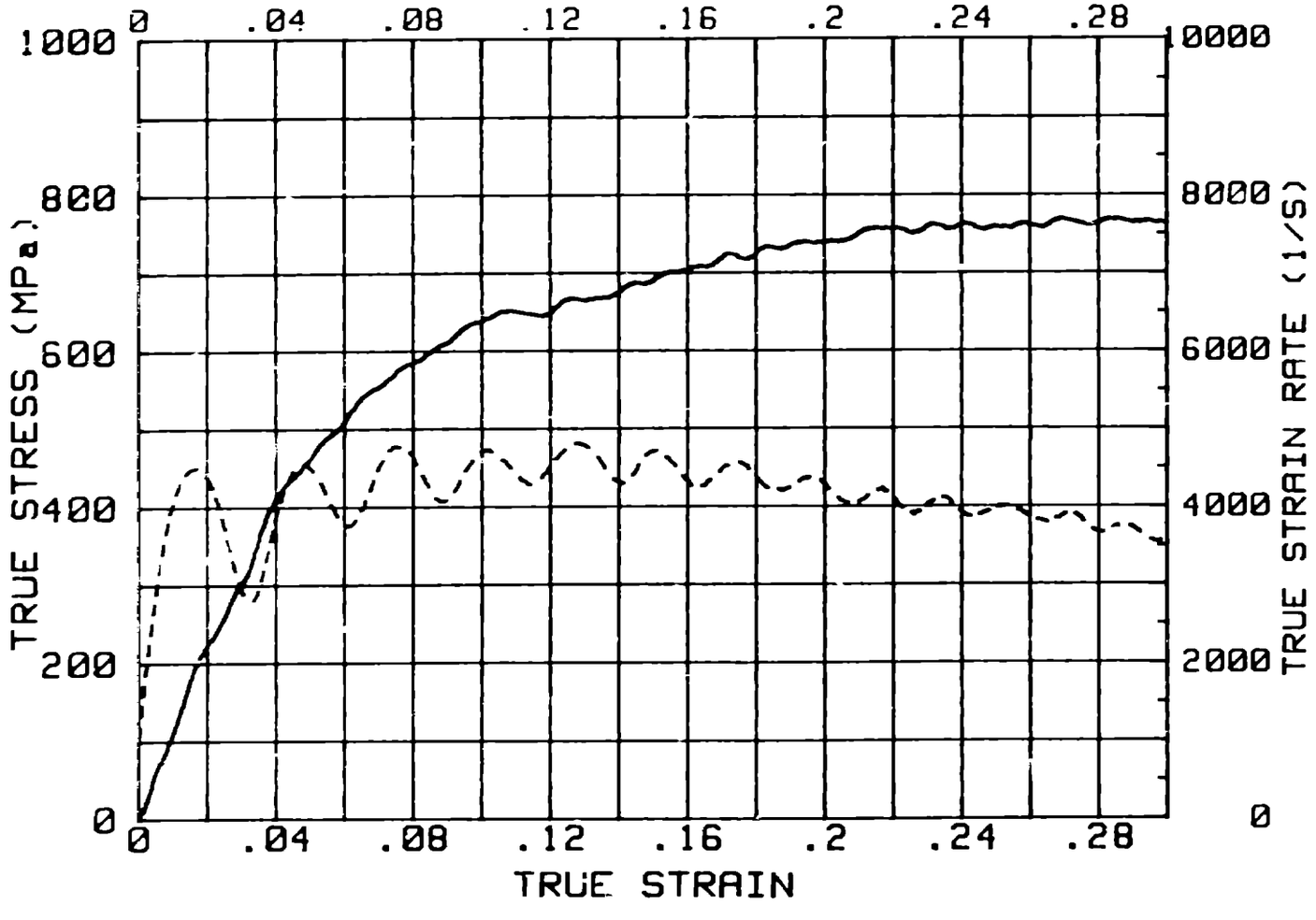
0
.04
.08
.12
.16
.2
.24
.28
1000
800
600
400
200
0
TRUE STRESS (MPa)
8000
6000
4000
2000
TRUE STRAIN RATE (1/S)
TRUE STRAIN